NeuroImage: Clinical 33 (2022) 102916

Contents lists available at ScienceDirect

NeuroImage: Clinical

journal homepage: www.elsevier.com/locate/ynicl

Aberrant functional metastability and structural connectivity are associated with rumination in individuals with major depressive disorder

Ruibin Zhang [a,1], Sammi-Kenzie T.S. Tam [b,c,1], Nichol M.L. Wong [b,c,*], Jingsong Wu [d], Jing Tao [d], Lidian Chen [d], Kangguang Lin [e,*], Tatia M.C. Lee [b,c,f,*]

[a] Laboratory of Cognitive Control and Brain Healthy, Department of Psychology, School of Public Health, Southern Medical University, Department of Psychiatry, Zhujiang Hospital, Southern Medical University, Guangzhou, China
[b] State Key Laboratory of Brain and Cognitive Sciences, The University of Hong Kong, Hong Kong, China
[c] Laboratory of Neuropsychology and Human Neuroscience, The University of Hong Kong, Hong Kong, China
[d] Fujian University of Traditional Chinese Medicine, Fuzhou, China
[e] Department of Affective Disorders, Guangzhou Huiai Hospital, The Affiliated Brain Hospital of Guangzhou Medical University, China
[f] Institute of Clinical Neuropsychology, The University of Hong Kong, Hong Kong, China

ARTICLE INFO

Keywords:
Rumination
Metastability
White matter integrity
Resting-state fMRI
Diffusion tensor imaging
Major depressive disorder

ABSTRACT

Rumination is a repetitive and compulsive thinking focusing on oneself, and the nature and consequences of distress. It is a core characteristic in psychiatric disorders characterized by affective dysregulation, and emerging evidence suggests that rumination is associated with aberrant dynamic functional connectivity and structural connectivity. However, the underlying neural mechanisms remain poorly understood. Here, we adopted a multimodal approach and tested the hypothesis that white matter connectivity forms the basis of the implications of temporal dynamics of functional connectivity in the rumination trait. Fifty-three depressed and ruminative individuals and a control group of 47 age- and gender-matched individuals with low levels of rumination underwent resting-state fMRI and diffusion tensor imaging. We found that lower global metastability and higher global synchrony of the dynamic functional connectivity were associated with higher levels of rumination. Specifically, the altered global synchrony and global metastability mediated the association between white matter integrity of the genu of the corpus callosum to rumination. Hence, our findings offered the first line of evidence for the intricate role of (sub)optimal transition of functional brain states in the connection of structural brain connectivity in ruminative thinking.

1. Introduction

Rumination is a pattern of recursive and compulsive thinking focusing on one's symptoms, causes, and consequences of distress (Nolen-Hoeksema et al., 2008; Papageorgiou and Siegle, 2003). Ruminators tend to have heightened risk of developing depressive episodes (Nolen-Hoeksema, 2000), making rumination a common symptom of disorders characterized by affective dysregulation (Kovács et al., 2020; Nolen-Hoeksema, 2000). Particularly, although a profile of aberrant brain structure and functional network organization has been found in mood disorders (for a review, see Bi and He, 2014; Gong and He, 2015; Liu et al., 2021), the specific underlying neural mechanisms of rumination remains elusive to date.

Past resting-state fMRI (rs-fMRI) studies mostly assumed brain connectivity to remain stationary over time (Park et al., 2018), which overlooks the temporal dynamics of functional alternations (Zhi et al., 2018), thereby, exploring the dynamics of resting-state functional connectivity could offer a fresh perspective on the neural functional aberrations subserving rumination.

Dynamic functional connectivity serves to measure the overall spatiotemporal organization of functional connectivity (Hansen et al., 2015). Its spatiotemporal structure as reflected by the complex spontaneous state-dependent changes in functional connectivity is thought to be associated with cognitive activities (Rabinovich et al., 2012). Among

* Corresponding authors at: Rm 656, The Jockey Club Tower, The University of Hong Kong, Pokfulam Road, Hong Kong, China (Tatia M.C. Lee). Department of Affective Disorder, Guangzhou Brain Hospital, 36 Mingxin Road, Guangzhou, Guangdong Province, China (K. Lin). Rm 658, The Jockey Club Tower, The University of Hong Kong, Pokfulam Road, Hong Kong, China (Nichol M.L. Wong).
E-mail addresses: nichol.wong@hku.hk (N.M.L. Wong), linkangguang@163.com (K. Lin), tmclee@hku.hk (T.M.C. Lee).
[1] Equal contribution.

https://doi.org/10.1016/j.nicl.2021.102916
Received 14 July 2021; Received in revised form 30 November 2021; Accepted 13 December 2021
Available online 14 December 2021

different measures of dynamic functional connectivity, particular focus has been placed on synchrony and metastability because they capture critical aspects of the dynamics building on the temporal patterns of the oscillatory activity of constituent brain regions (Cabral et al., 2011; Pedersen et al., 2018b). Synchrony is a measure of mean phase coherence over time which underpins information exchange (Fries, 2015; Pajevic et al., 2014), while metastability represents the variability in the synchronization of network regions over time and is considered important for adaptive information processing and cognitive flexibility (Alderson et al., 2020; Tognoli and Kelso, 2014). In the present study, we studied these two dynamic properties as metrics of dynamic connectivity.

Rumination leads to highly negative thinking and narrows down the attention scope, resulting in decreased action repertoires and increased likelihood of biased and self-related thoughts (Whitmer and Gotlib, 2013). This habit of inflexible, sustained attention to self-referential information can be reflected by abnormal dynamic connectivity (Kaiser et al., 2016; Wise et al., 2017). Theoretically speaking, neural synchrony and affective dysregulation could be closely linked to each other (Uhlhaas and Singer, 2006), though, this has yet to be directly tested in the framework of rumination. Preliminary evidence has reported that reduced metastability is associated with higher self-reported depression severity (Kaiser et al., 2016; Martínez et al., 2020), with individuals with major depressive disorder (MDD) spending more time in a ruminative state compared to controls (Rosenbaum et al., 2017), these findings thus warrant the speculation that impaired synchrony and metastability could be associated with higher levels of rumination.

There is a paucity of research examining the association between white matter abnormalities and rumination but limited existing findings have found support (Borchers et al., 2019; Zuo et al., 2012), with some found a strong negative correlation between white matter integrity of the corpus callosum and rumination (e.g., Pisner et al., 2018). Furthermore, altered structural connectivity in the frontal-limbic-subcortical circuitry has been noted among mood disorders (Lisy et al., 2011; Lu et al., 2017). For example, greater alteration in the white matter circuits connecting the prefrontal lobe, the parietal lobe, and the limbic system could be associated with a more ruminative state (Zuo et al., 2012), potentially because damaged connectivity in brain structures may limit the dynamic repository available (Deco and Kringelbach, 2016).

Particularly, emerging evidence presenting the constraints structural connectivity could impose on the brain functional outcomes, such as that of dynamic functional connectivity (Liégeois et al., 2016; Park et al., 2017); and on behavioral functional outcomes (de Schotten et al., 2020; Penke et al., 2012) lends further support to the proposition that structural connectivity may be a basis of the dynamicity of functional connectivity and thereafter subserving rumination. We were not aware of any study examining whether brain metastability is critical to the implication of white matter integrity in rumination. Therefore, studies interrogating the mediating role of altered repertoire of brain dynamics could be important to foster understanding on structural integrity and dynamic connectivity subserving rumination.

To this end, we investigated the implication of structural connectivity and dynamic functional connectivity in rumination in individuals with MDD and healthy controls, and assessed how both types of connectivity are related to their rumination via a multimodal approach. Rumination is a common feature in disorders categorized by affective dysregulation (Kovács et al., 2020), the strong association between rumination and depression in particular has thus rendered this MDD patient population an ideal sample (Nolen-Hoeksema, 2000; Nolen-Hoeksema et al., 2008). We hypothesized that white matter integrity captured in diffusion tensor imaging (DTI) data, and the global synchrony and global metastability captured in rs-fMRI data would be significantly different between the two groups. We also investigated whether brain metastability could explain the statistical prediction of structural integrity of white matter on levels of rumination.

2. Materials and methods

2.1. Overview

The analysis protocol was composed of three parts. Briefly, we obtained global synchrony and global metastability values in our participants from the analytic signals of their rs-fMRI data (Fig. 1A–J). We also estimated their white matter integrity with tract-based spatial statistics (TBSS) and investigated its association with metastability (Fig. 1K). Finally, we investigated the relationships among structural connectivity, global synchrony, global metastability, and rumination using a mediation model. Analytic signals can be used to investigate neuronal synchronization (Glerean et al., 2012; Pedersen et al., 2018a) with superior association with brain structure (Ponce-Alvarez et al., 2015) – the white matter integrity under investigation, thereby, they can provide insights into the relationship between brain structure and abnormalities in brain function – rumination in the present study. Analytic signal-based functional connectivity is one method used to ascertain functional connectivity premised on the band-pass-filtered time series and can be employed to characterize unique time-varying connectivity networks (Calhoun et al., 2014). Processing of the analytic signals derived from rs-fMRI data will be further explained in the following sections.

2.2. Participants

The initial sample consisted of 100 right-handed participants including 53 individuals with major depressive disorder (MDD) and a control group of 47 age- and gender-matched individuals without MDD (MDD: 31 female, 22 male; Control: 27 female, 20 male). Participants were aged between 19 and 57 years old. Individuals with MDD were diagnosed according to the criteria of Diagnostic and Statistical Manual of Mental Disorders (DSM-V) (Uher et al., 2014) by their case psychiatrists. All MDD individuals had 17 or more scores on the Hamilton Depression Rating Scale 21-item inventory (HAM-D21; Cusin et al., 2009; Hamilton, 1986). The exclusion criteria were Axis-I psychiatric disorders other than MDD, Axis-II psychiatric disorders, history of organic brain disorders, neurological disorders, mental retardation, cardiovascular diseases, alcohol or substance abuse, pregnancy, or any physical illnesses. No participants received electroconvulsive therapy within six months before data collection, and all individuals with MDD were on stable antidepressant treatments before MRI scanning (Table 1).

Control group participants without MDD were recruited through local advertisements and screened using the Structured Clinical Interview for DSM-V (Nonpatient Edition) to rule out the presence of current or past psychiatric disorders. Further exclusion criteria were any history of psychiatric disorders in first-degree relatives, and current or past significant medical or neurological illnesses.

All individuals self-reported as right-handed, and no brain abnormalities were found on conventional MRI by an experienced radiologist. All participants completed MRI scanning within one week of clinical diagnosis and provided written informed consent. They were compensated for their participation (¥150). Ethical approval was obtained from the Institutional Review Board of Guangzhou Brain Hospital. All experimental procedures were conducted in accordance with the Declaration of Helsinki (1975).

2.3. Behavioral assessment

Rumination was assessed with the Ruminative Response Scale (RRS; Treynor et al. 2003). RRS is a self-reported assessment often used to measure rumination. It consists of 22 items with three subcomponents: depression, brooding, and reflection rated on a 4-point Likert scale (i.e., never, sometimes, often, always). RRS has been shown to be a reliable and valid measure of rumination in the Chinese population, $\alpha = 0.90$ (Han and Yang, 2009).

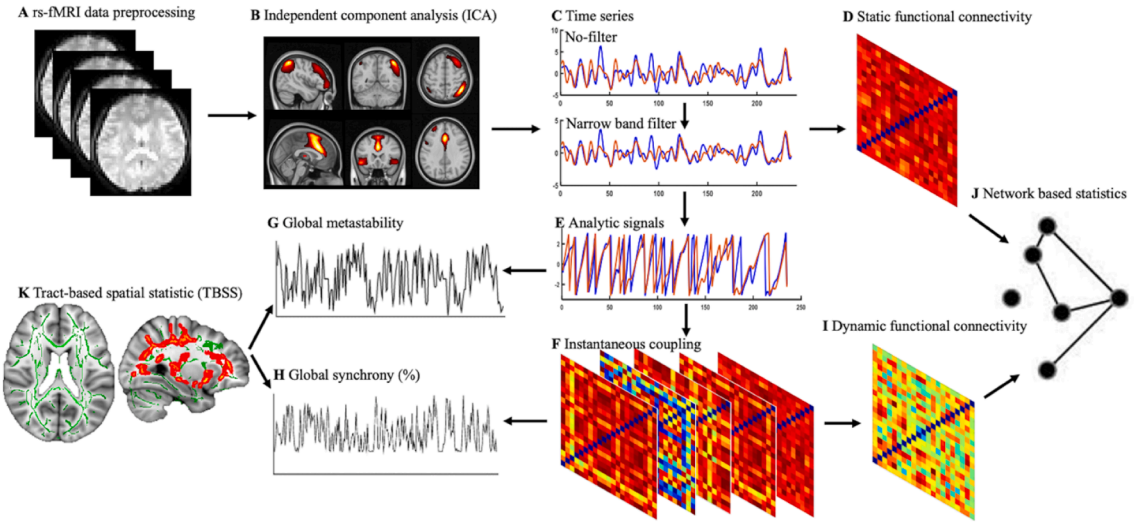

Fig. 1. Data analysis flowchart. (A) Resting-state fMRI (rs-fMRI) data preprocessing. (B) Group-independent component analysis (ICA). (C) Extracting time series of each component and filtering with narrow band (0.04–0.07 Hz). (D) Estimating the static functional connectivity using Pearson correlation. (E, F) Deriving the analytic signals of each component and estimating the instantaneous phase coupling at each time point. (G, H) Estimating global metastability and global synchrony. (I) Constructing the dynamic functional connectivity using coefficient of variation. (J) Network based statistics (NBS) analysis revealing the inter-component connectivity difference. (K) Tract-based spatial statistics analysis (TBSS) in DTI data.

Table 1
Demographical and clinical variables.

	MDD individuals	Controls without MDD	t / X^2 statistics
Age	31.90 (9.96)	28.93 (10.88)	$t = 1.43$, $p = 0.15$
Sex	31F / 22M	27F / 20M	$X^2 = 0.01$, $p = 0.92$
Edu	12.88 (3.51)	13.46 (3.16)	$t = -0.87$, $p = 0.38$
HAM-D21	33.59 (8.17)	2.10 (3.57)	$t = 24.43$, $p < 0.001$
Power FD	0.10 (0.05)	0.11 (0.06)	$t = -1.48$, $p = 0.15$
RRS total	57.42 (11.26)	37.53 (9.23)	$t = 9.61$, $p < 0.001$
RRS_Depression	30.74 (6.65)	18.95 (5.15)	$t = 9.84$, $p < 0.001$
RRS_Brooding	14.59 (3.03)	9.57 (2.66)	$t = 8.77$, $p < 0.001$
RRS_Reflection	11.91 (3.04)	9 (2.38)	$t = 5.27$, $p < 0.001$

MDD = major depressive disorder; Edu = years of education; HAM-D21 = Hamilton Depression Rating Scale (21-item); FD = framewise displacement; RRS = Ruminative Response Scale ; F = female; M = male.
Means with standard deviations in parentheses are presented, except for sex ratio.

2.4. Imaging data acquisition and preprocessing

All neuroimaging data were acquired on a 3.0 Tesla MR imaging system (Achieva X-series, Philips Medical Systems, Best, Netherlands) with an eight-channel SENSE head coil at the Department of Radiology, Guangzhou Brain Hospital, China. Tight but comfortable foam padding was used to reduce head motion, and earplugs were used to muffle scanner noise.

Resting-state fMRI images were acquired using a gradient-echo echo-planar imaging (GRE-EPI) sequence with repetition time (TR) = 2000 ms, echo time (TE) = 30 ms, flip angle = 90°, matrix = 64 × 64, field of view (FOV) = 220 mm × 220 mm, slice thickness = 4 mm with interslice gap = 0.6 mm, 33 interleaved axial slices, and 240 time points. T1-weighted images (MRI) were acquired with an interleaved sequence (188 sagittal slices, TR/TE/flip angle = 8.2 ms/3.7 ms/7°, matrix = 256 × 256 mm^2, FOV = 256 × 256 × 188 mm, voxel size = 1 × 1 × 1 mm^3). The DTI images were collected with these parameters: 32 diffusion-weighted (b = 1000 sec/mm^2) and 1 non-diffusion weighted scans; TR = 10100 ms; TE = 90 ms, FOV = 256 × 256 mm^2, voxel size = 2 × 2 × 2 mm^3.

The fMRI data were preprocessed using Statistical Parameter Mapping (SPM 12, http://www.fil.ion.ucl.ac.uk/spm, Wellcome Trust Centre for Neuroimaging, London, UK) and Data Processing & Analysis for (Resting-State) Brain Imaging (DPABI, v6.0, http://rfmri.org/dpabi; Yan et al., 2016) with a standard pipeline, including correction for slice timing and motions, normalization of functional volumes using T1-weighted images, resampling to 3-mm isotropic voxels, and smoothing with 6-mm kernel. Moreover, we regressed out the Friston-24 parameters of head motion (six head motion parameters, six head motion parameters at one time point before, and the twelve corresponding squared items) (Power et al., 2012; Satterthwaite et al., 2013), as well as signals of the white matter and cerebrospinal fluid.

We obtained global signal by averaging all brain voxels' time series and calculated the number of voxels that negatively correlated with the global signal. We then computed Global Negative Index (GNI) with the following formula (Chen et al., 2012; Fox and Raichle, 2007):

$$\mathrm{GNI} = \frac{No.\ of\ voxels\ negatively\ correlated\ with\ global\ signal\ (p < 0.05,\ uncorrected)}{Total\ no.\ of\ voxels}.$$

GNI was calculated to assess whether global signal regression should be performed or not. If the GNI is < 3%, performing global signal regression induces less error, therefore, it is highly recommended that the global regression should be performed. If GNI is > 3%, performing global signal regression induces more errors. In this study, global signal regression was not performed after the examination of GNI profiles as all participants were found to have a GNI > 3%.

We also looked at the Power frame displacement (FD). If FD of any

particular time point of the fMRI data is > 0.5, that time point is considered a "bad" time point, and the time points before and after that bad time point will be scrubbed using each of the bad time points as a regressor (Power et al., 2012). We excluded four participants who had displacement ≥ 3 mm in any plane and rotation ≥ 3° in any direction in their fMRI data. Hence, a total of 51 individuals with MDD and 45 age- and gender-matched control individuals without MDD were included in the final data analyses. A more detailed description of the preprocessing of fMRI data is reported in the Supplementary Information.

For DTI data, standard preprocessing was applied using the FMRIB's Diffusion Toolbox (FDT, v6.0, https://fsl.fmrib.ox.ac.uk/fsl; Smith et al., 2004) implemented in FMRIB Software Library (FSL) to obtain the fractional anisotropy (FA) diffusion maps. Briefly, the DTI images were first corrected for eddy current and the motion between images. The gradient directions for rotations were subsequently adjusted, followed by the removal of non-brain tissue. Diffusion metrics maps, including FA and eigenvector maps were then estimated and inspected visually for orientation and image quality. FA diffusion maps were subsequently skeletonized and transformed into common space, all FA volumes were then warped to the template through FMRIB's non-linear image registration. The mean FA images of all individuals were thinned to create a mean FA skeleton representing the centers of all white matter tracts, and were binarized at FA = 0.3. Individual FA values were then warped onto the mean FA skeleton.

2.5. Independent component analysis and dynamic functional connectivity

We conducted a spatial independent component analysis (ICA) using the preprocessed fMRI data in Group ICA of fMRI Toolbox (GIFT toolbox, v4.0b, http://mialab.mrn.org/software/gift/; Calhoun et al., 2001). Spatial ICA decomposed data from each participant into linear mixtures of spatially independent components exhibiting a unique time course profile. Principal component analysis (PCA) was applied to reduce data dimensionality for each participant. Then, reduced data from all participants were concatenated and subjected to a second-data reduction step using PCA. The number of independent group components was set at 23, which was based on the minimum description length criterion. The reliability of the independent component decomposition was tested by running Infomax 20 times in the Software for Investigating the Reliability of ICA Estimates by Clustering and Visualization (Icasso package, v1.22, https://research.ics.aalto.fi/ica/icasso/abouthttps://research.ics.aalto.fi/ica/icasso/; Himberg et al., 2004). Finally, individual subject components for each participant were reconstructed back from the group components using the group ICA approach, during which the aggregated components and results from the data reduction step were utilized to compute individual subject components.

Subject-specific spatial map and time series of each participant were processed further with the following steps. First, we obtained one sample *t*-test maps for each spatial map across all participants and merged these maps to obtain regions of peak activation clusters for that component using SPM12, $p < 0.01$, cluster size > 100 voxels, and family-wise error correction. An average of blood-oxygen-level-dependent (BOLD) signals was computed across each component. Thus, a series of components represented intrinsic connectivity networks when their peak activation clusters fell on the gray matter. Theydemonstrated minimal overlap with known vascular, susceptibility, ventricular, and edge regions that corresponded to head motion. Following the recommendation of Kelly et al. (2010), two components were removed after visual screening, thereby resulting in 21 ICs' time-series data in the final analyses (Fig. 2).

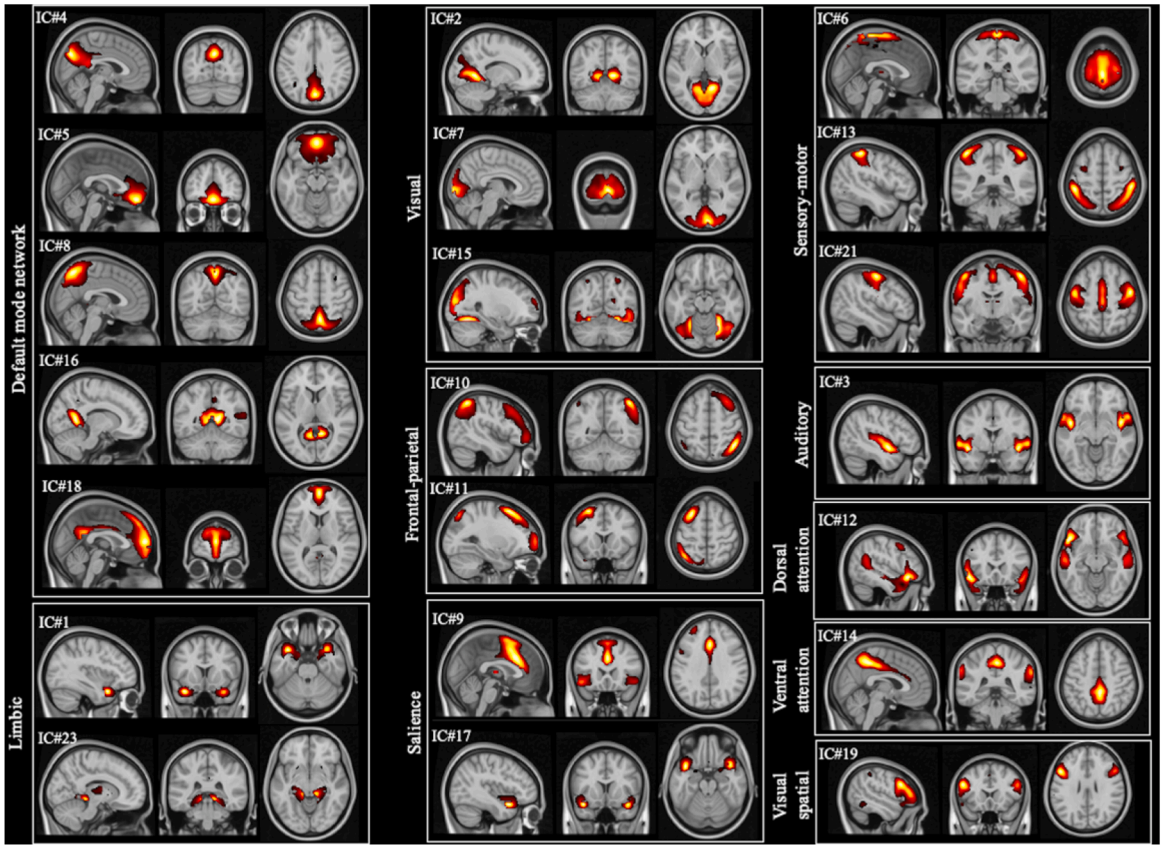

Fig. 2. Identified components by independent component analysis (ICA). 10 networks derived from 21 ICs' time-series data.

2.6. Functional connectivity construction

The subject-specific time series corresponding to the ICs for each participant were extracted and band-pass filtered between 0.04 and 0.07 Hz into analytic signals using the Hilbert transformation (Glerean et al., 2012) for subsequent static and phase-based dynamic functional connectivity estimation and analyses. This narrow frequency range has been found to be reliable and optimal for examining BOLD analytic signal patterns (Pedersen et al., 2018a). The static functional connectivity was defined as the Pearson correlation coefficient (r) between time series of each component and the coefficients were approximated as a normal distribution.

The analytic signals derived from the 21 ICs' time-series data can be understood as the product of two properties: instantaneous phase and instantaneous envelope (Glerean et al., 2012; Lachaux et al., 1999). Accordingly, functional connectivity profiles can be constructed using an analytic representation by means of the instantaneous phases. This phase-based method provides an alternative way to characterize dynamic functional connectivity with higher temporal resolution given the short duration of a resting-state fMRI session (Glerean et al., 2012). Ponce-Alvarez et al. (2015) has illustrated the use of this method to detect community structures and compared it with well-established methods such as the ICA. Moreover, the functional connectivity profiles derived from this approach has been found to be a reliable fingerprint for identifying individuals more than two years after (Zhang et al., 2019).

Briefly, the analytical signals were computed according to previous work (Glerean et al., 2012; Zhang et al., 2019) and its formula can be expressed as follows, with H[.] as the Hilbert transformation, i as the imaginary unit, and the new signal $x_{a(t)}$ has the identical Fourier transformations $x(t)$, despite being defined only for positive frequencies:

$$x_{a(t)} = x(t) + iH[x(t)]$$

Similarly, let $x(t)$ be expressed as an amplitude signal $\mathrm{a}(t)$ with carrier frequency $\varnothing(\mathrm{t})$, thus:

$$x(t) = a(t)\cos[\varnothing(t)].$$

Then Hilbert transformed analytic signal can be written as the product of two meaningful components:

$$x_{a(t)=}a(t)e^{i\varnothing(t)},$$

where $|a(t)|$ represents the instantaneous envelope and $\varnothing(t)$ is the instantaneous phase.

Pairwise instantaneous phase differences at each time point among components were computed to reflect instantaneous phase coupling of the dynamic functional connectivity. Pairwise estimates of dynamic phase (de)coupling were estimated as follows, for each time instance t, the pairwise difference in phase between the time-series i and time series j was computed as:

$$\Delta\varnothing_{ij} = \begin{cases} \left|\varnothing_i(t) - \varnothing_j(t)\right|, if \left|\varnothing_i(t) - \varnothing_j(t)\right| \le \pi \\ 2\pi - \left|\varnothing_i(t) - \varnothing_j(t)\right|, otherwise \end{cases}.$$

Then, instantaneous coupling matrices, $C(t)$ were constructed using phase differences normalized between 0 and 1, thereby respectively representing perfect anti-synchronization and perfect synchronization, such that:

$$C_{ij}(t) = 1 - \frac{\Delta\varnothing_{ij}(t)}{\pi}.$$

The coefficient of variation (variance/mean) of each element $C_{ij}(t)$ across all time points is the final pairwise metric of phase coupling/de-coupling.

This approach has been proven to be a stable and reliable dynamic functional fingerprint for identifying individuals with a high success rate of 86% ($p < 0.001$), indicating that instantaneous phase as an analytic signal may serve as a contemporary and promising tool for the study of dynamic functional connectivity. For details, refer to our previous work (Zhang et al., 2019).

2.7. Dynamic functional connectivity

We used two metrics, global synchrony and global metastability, to capture the dynamic properties of functional connectivity. The biological mechanisms supporting these network properties occur at multiple timescales, including the slow frequencies measured with fMRI (Ponce-Alvarez et al., 2015).

2.7.1. Global synchrony

Global synchrony was calculated using binarized instantaneous coupling matrices (ICMs) (i.e., binary connectivity matrices ($C^b(t)$) composed of phase differences between components $< \pi/8$, a benchmark for determining binary connectivity):

$$C^b(t) = \begin{bmatrix} C^b_{ij}(t) = 1, if \Delta\varphi_{ij} < \pi/8 \\ C^b_{ij}(t) = 0, otherwise \end{bmatrix}.$$

The final matrix of dynamic functional connectivity consisted of an ICM at each time point, wherein the percentage of existing connections at each binary ICM (as each time point yielded a percentage of synchronized pairs) was determined as global synchrony, a measure of general coherence of instantaneous phases. The coefficient of variation of each matrix across all time points is the final pairwise metric of phase coupling/de-coupling. N represents the number of components in the formula provided below:

$$G(t) = 100\left(\frac{\sum_{i,j\in N} C^b_{ij}(t)}{\frac{N!}{(N-2)!2!}}\right).$$

The average global synchrony ($\overline{G}$) across all time points was subsequently computed for each participant (detailed formula and explanations were given in a former work [Demirtaş et al., 2016]). A high $\overline{G}$ indicates that the participant tends to linger in a state where the overall phase-coupling among oscillators is persistently high.

2.7.2. Global metastability

Global metastability was computed as the standard deviation of the Kuramoto order parameter (a proxy for instantaneous whole-brain synchrony) $R(t)$, shown as follows:

$$R(t) = \frac{1}{N}\sum_{k=1}^{N} e^{i\varnothing_k(t)},$$

where $k = [1\ldots, N]$ stands for the oscillators (here, $N = 21$ ICA-derived components), and $\varnothing_k(t)$ is the instantaneous phase of the k-th oscillator (time-series) at time t. Metastability provides a measure indicating the global level of synchrony of oscillating signals.

2.7.3. Network-based statistic (NBS) analysis

In addition to global measures of dynamic functional connectivity, to evaluate measures of network dynamics, we also looked into edge-wise level of dynamic that focuses on time-series clustering which are known to have time and spatial correlations (Harrington et al., 2015). NBS aims to identify connected components in brain graph by transforming time series from time-space domain to topographical domain, and to find groups of time series that are similar within a cluster (intra-cluster similarity) but are comparatively different from that of other clusters (inter-cluster similarity) to form network representations (Ferreira and Zhao, 2016). Group comparisons in functional connectivity between individuals with MDD and healthy controls using this approach were not

the focus of this study and more details are reported in Supplementary Information (Fig. S2). In brief, we calculated the variability (variance/mean) of the phase coupling between each binary pair (0 and 1) across time, indexed as the variability of instantaneous phase coupling, and computed separate mean synchrony and metastability measures for the phase time series of components within the 10 networks defined. Connectivity matrices were entered as between-subject dependent variables into the NBS toolbox to identify functional connections (Zalesky et al., 2010), including the static and dynamic functional connectivity that showed group differences. Across the groups, the components identified using this method were extracted as components of interest. The primary threshold of individual-connection level was set at $p < 0.01$ with extent-based correction for multiple comparisons, 5,000 permutations, and an overall corrected $\alpha < 0.05$. Age and gender were regressed out as covariates.

2.8. Surrogate time series

Surrogate time series under linearity and stationarity assumption were estimated to check whether the observed measures were due to dynamics (Prichard and Theiler, 1994). They were produced before band-pass filtering using the constrained phase randomization approach. Overall, 100 surrogates were generated for each participant, which mimicked the autocorrelations of each variable (time series) and the cross-correlations among all variables. The correlation coefficients, mean, and variance of the phase coupling values between components were preserved in the surrogate signals. Group averages for $\overline{G}$ and metastability were estimated using 1,000 values that were randomly sampled from the surrogates, and the *p*-value was calculated as the probability of the observed test statistic under this estimated null distribution. Therefore, the null hypothesis would be rejected when the *p*-value was < 0.05. The observed statistic was defined as the *t*-value for group comparisons.

2.9. Relationship between white matter integrity and dynamic functional connectivity

Since neural activity synchrony among different brain areas provides a flexible switch for different routes of effective communication while maintaining the fixed skeleton of structural connections (Deco and Kringelbach, 2016), we investigated the structural connectivity basis of aberrant dynamic connectivity. White matter integrity, as indexed by FA values, characterizes the strength of structural connectivity under study.

2.10. Relationship between dynamic functional connectivity and clinical variables

We examined the relationships between dynamic properties showing significant between-group differences and clinical variables, including HAM-D21 scores, age of onset of depression, duration of depression, and rumination scores.

2.11. Mediation analyses

We performed mediation analyses to gain insight into the extent to which alterations in dynamic functional connectivity could explain the association between structural connectivity alterations and rumination in individuals. Specifically, we tested whether global synchrony and global metastability would mediate the relationship between white matter integrity and rumination.

3. Statistical analyses

3.1. Group comparison in white matter integrity

Voxel-wise TBSS with permutation tests on the final FA skeleton was conducted to identify differences in white matter integrity between individuals with MDD and the control group using the FSL/RANDOMISE tool (5,000 permutations), controlling for age, gender, and age × gender interaction. We included these covariates in our analyses due to the large age range of our participants and because previous studies suggested that age and gender should be controlled for in functional connectivity studies (Sie et al., 2019; C. Zhang et al., 2016).

3.2. Group comparison in dynamic functional connectivity

A non-parametric permutation test was employed to assess the statistical significance of between-group differences (i.e., MDD individuals vs. control group). Randomization with 5,000 permutations was performed for global synchrony and global metastability, and the corresponding distribution of the *t*-statistics was obtained. Age, gender, and age × gender interaction terms were included as covariates.

3.3. Relationship between white matter integrity and dynamic functional connectivity

We first extracted FA values from the TBSS-derived white matter skeleton which showed significant group differences. As no group × FA effects on the dynamic properties were observed, we then estimated the Pearson correlation between FA values and dynamic properties to evaluate whether alterations in white matter integrity of specific areas was related to the aberrant dynamic connectivity observed. Age, gender, and age × gender interaction terms were included as covariates. Instead of Pearson's *r*, *t*-values were reported as an alternative statistic charting the association between the independent variable and dependent variable, i.e., the white matter integrity and dynamic functional connectivity.

3.4. Relationship between dynamic functional connectivity and clinical variables

For global synchrony and global metastability showing significant between-group differences, we further performed multiple linear regression analyses to examine the relationships between these and clinical variables, controlling for age, gender, and age × gender interaction. Similarly, *t*-values were reported as an alternative statistic charting the association between dynamic functional connectivity and clinical variables.

3.5. Mediation analyses

The mediation analyses were conducted in R (v3.5.3) using the script written by Tingley et al. (2014), where prefrontal white matter integrity (FA value), metrics of dynamic connectivity (global synchrony and global metastability), and rumination (RRS) were defined as the independent variable, the proposed mediator, and the dependent variable, respectively. To test whether paths in the mediation model fit well, bootstrapping with 5,000 samples was performed, if 0 did not fall within the 95% confidence interval of estimated coefficients (i.e., *a* is the path coefficient of independent variable to mediator, *b* is the path coefficient of mediator to dependent variable controlling for the effect of independent variable, *c'* is the direct effect of independent variable to dependent variable controlling for the effect of mediator, and *c* is the total effect from independent to dependent variable), the estimate was deemed statistically significant. Of note, group (MDD individuals vs. control group), age, gender, and age × gender interaction terms were included as covariates. *T*-values were also reported as an alternative

statistic charting the association between global synchrony and rumination, as well as between global metastability and rumination.

3.6. Data and code availability

The datasets reported in this manuscript are not publicly available due to the lack of informed consent from participants and ethical approval for public data sharing. Custom code that supports the findings of this study is available upon reasonable request from the corresponding authors.

4. Results

4.1. Demographic and clinical variables

There were no significant differences between two groups in age, gender, or years of education ($p > 0.05$), confirming that individuals with MDD and control group individuals were matched on demographics. As expected, individuals with MDD showed significantly higher scores than the control group in all administered clinical assessments, including rumination (i.e., HAM-D21, RRS; $p < 0.05$; Table 1).

4.2. White matter integrity alterations

Standard TBSS analysis was performed to compare individuals with MDD to the control group on white matter integrity as indexed by FA values, with age, gender, age × gender as covariates of no interest. Compared to the control group, widespread reduction in FA was found across the white matter skeleton in individuals with MDD ($p < 0.05$, threshold-free cluster enhancement [TFCE] corrected; Fig. 4A, Table 2). In particular, FA reduction was the largest in the corpus callosum, the tracts within the bilateral superior longitudinal fasciculus, and the anterior and posterior limbs of the internal capsule. A significant reduction in FA was also observed in the posterior and anterior parts of the corona radiata. However, brain clusters with increased FA values were not evident in individuals with MDD when compared to control group individuals ($p > 0.05$).

Table 2
The anatomical areas that showed significantly reduced fractional anisotropy (FA) values in MDD individuals compared to controls (threshold-free cluster enhancement [TFCE] corrected, $p < 0.05$).

Cluster	Cluster size	Anatomical region (proportion[a])	MNI X	Y	Z	t-value
1	9213	Genu of corpus callosum (26%); Anterior corona radiate. R (17%); Anterior corona radiate. L (17%)	−18	27	13	4.87
2	3483	Superior longitudinal fasciculus. R (78%); Posterior corona radiate. R (21%)	25	−56	29	3.89
3	3366	Splenium of corpus callosum (38%); Body of corpus callosum (32%); Posterior corona radiate. L (14%)	−32	−41	34	3.59
4	3287	Posterior thalamic radiation. R (38%); Retrolenticular part of internal capsule. R (19%)	34	−21	−8	4.06
5	2079	Superior longitudinal fasciculus. L (68%); Superior corona radiate. R (28%)	−32	−14	38	4.70
6	660	External capsule. L (33%); Retrolenticular part of internal capsule. L (22%)	−33	−14	−12	4.01
7	216	Retrolenticular part of internal capsule. L (33%)	−46	−38	−3	2.87

L/R = left/right hemisphere.
Anatomical regions were defined by Johns Hopkins University DTI-based White Matter Atlas.
[a] Proportion represents the relative distribution of voxels if the clusters map into atlas.

4.3. Aberrant dynamic functional connectivity

Global synchrony increased significantly in individuals with MDD compared to the control group ($t = 2.22$, $p = 0.024$; Fig. 3A). Furthermore, a significant difference was also found between the means of global metastability, with lower metastability found among those with MDD than in control group participants ($t = 2.14$, $p = 0.019$; Fig. 3B). Further analysis on the network level revealed no significant difference between the two groups at the subnetwork level ($p > 0.05$). These results suggested less flexibility and substantial stability of dynamic functional connectivity in depressed individuals with high levels of rumination (Demirtaş et al., 2016).

4.4. Surrogate time series

Next, we tested the hypothesis that the group averages of dynamic connectivity were linear and stationary. The null hypotheses were rejected both for global synchrony ($p < 0.001$; Fig. 3C) and global metastability ($p = 0.001$; Fig. 3D).

4.5. Association between white matter integrity alterations and aberrant dynamic functional connectivity

We further investigated whether differences in white matter integrity were related to global synchrony and global metastability. We calculated mean FA values across the white matter skeleton and within the white matter mask which revealed group differences in global synchrony and global metastability. We found significant associations between FA values and global synchrony ($t = -2.08$, $p = 0.040$), and between FA values and global metastability ($t = 2.36$, $p = 0.020$; Fig. 4B) after controlling for group differences. Separately within each group, we also performed a voxel-wise regression of global synchrony and global metastability on FA to address the relationships at the voxel-wise level ($p < 0.05$, TFCE corrected). A significant positive association was observed between global metastability and integrity of the white matter skeleton, largely within the white matter linking the bilateral prefrontal lobe and the genu of the corpus callosum (Fig. 4C, D).

4.6. Association between aberrant dynamic functional connectivity and rumination

We examined whether global synchrony and global metastability would be related to rumination (i.e., total RRS and subscale scores), controlling for group, age, gender, and age × gender interaction. Group was further included as a covariate to control for group differences in global synchrony, global metastability, FA values, and voxel-wise regression of global synchrony and global metastability on FA. Global synchrony presented a significantly positive relationship ($t = 2.71$, $p = 0.008$; Fig. 5A), whereas global metastability exhibited a significantly negative relationship with total RRS scores ($t = -2.33$, $p = 0.022$; Fig. 5B). However, no significant associations were detected between global synchrony or global metastability and depression severity ($p_s > 0.05$).

4.7. Aberrant dynamic functional connectivity mediated the association between prefrontal white matter integrity and rumination

First, we found that FA value demonstrated a significant effect in its prediction of rumination when group is being controlled for ($c =$

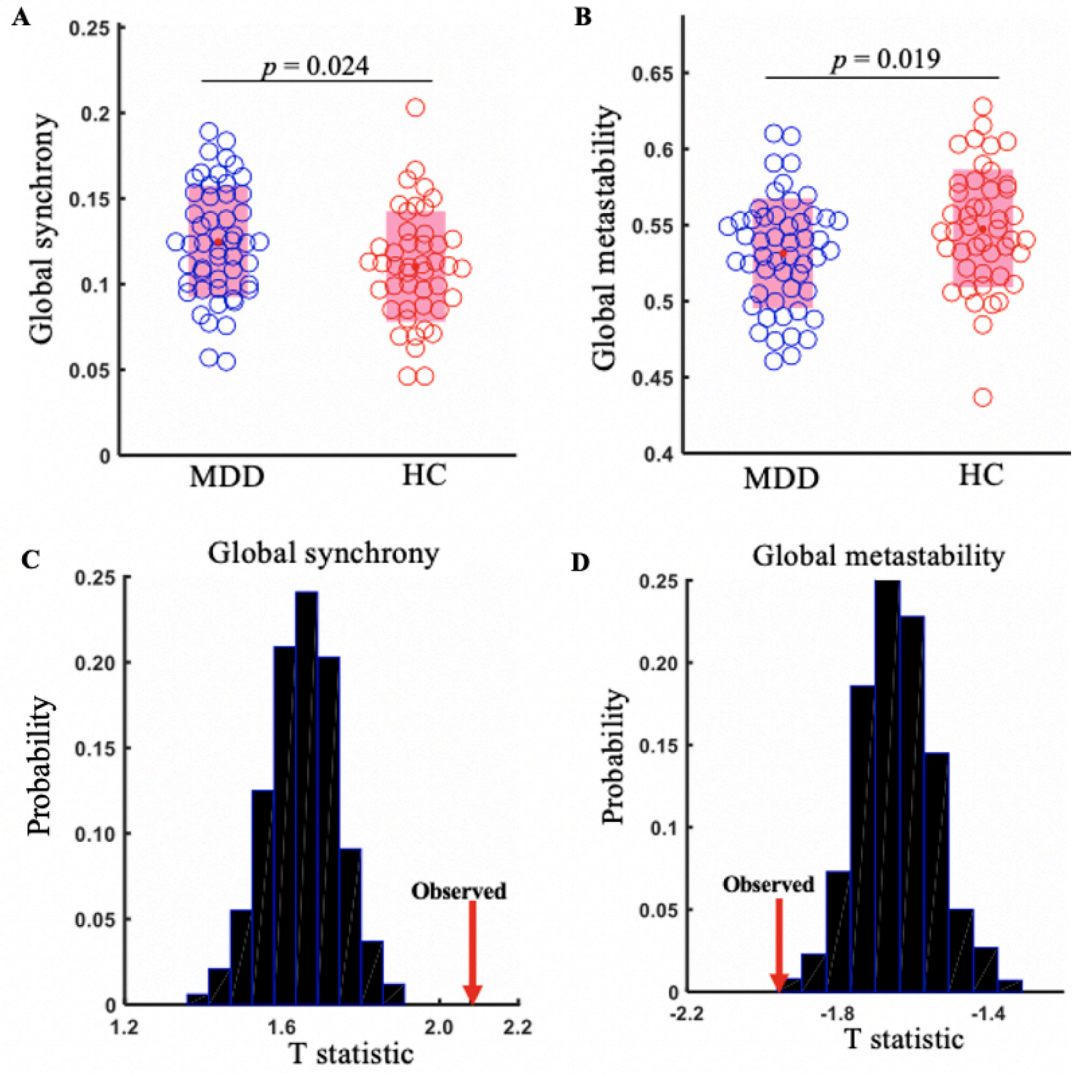

Fig. 3. Analysis of dynamic functional connectivity. (A) Increased global synchrony in individuals with major depressive disorder (MDD) compared to healthy controls. (B) Decreased global metastability in individuals with MDD than controls. (C) Global synchrony test statistics calculated using multivariate surrogate data. (D) Null distributions of global metastability. Red arrows indicated observed test statistics.

-356.02, t = -5.05, $p < 0.001$). We then further examined whether dynamic connectivity played a role in the relationship between white matter integrity and rumination using a mediation model, with group being controlled for. We used the bootstrapping method to test the indirect effects of global synchrony (ab = -46.52, 95%CI [-113.67, -3.52], $p = 0.026$) and global metastability (ab = -37.08, 95%CI [-94.7, -0.91], $p = 0.042$) (Fig. 5C). Results revealed that bilateral prefrontal white matter integrity had significant indirect effects on rumination via global synchrony and global metastability, with the indirect effects of global synchrony and global metastability respectively accounting for approximately 13.7% and 10.4% in the mediation. Mediation results of the RRS subscales are presented in Table S2.

5. Discussion

To the best of our knowledge, this study is the first to investigate the role of dynamic functional connectivity in mediating the association between structural connectivity and rumination. Studying global synchrony and global metastability as two dynamic properties of resting-state functional connectivity, we found that individuals with MDD, characterized by higher rumination, have high global synchrony and low global metastability, and this was related to altered white matter integrity of the genu of the corpus callosum interconnecting bilateral prefrontal regions. Specifically, the dynamic connectivity mediated the close association between structural integrity in white matter of the bilateral prefrontal cortex and rumination. Our findings offered the first line of evidence that brain metastability is associated with rumination, which has its basis in altered white matter connectivity.

5.1. Decreased brain metastability is associated with rumination

The brain functional connectivity is highly dynamic (Liu et al., 2018; Váša et al., 2015). We utilized phase-based dynamic functional connectivity as this approach could improve temporal resolution using each time point as a unit (Glerean et al., 2012), and allow us to measure metastability as an essential property of neural activity (Deco and Kringelbach, 2016). In addition, dynamical functional connectivity derived from phases could address a significant proportion of the association between brain structure and function (Ponce-Alvarez et al., 2015), and explain in part the brain deficits in psychopathology (Hellyer et al., 2015).

Metastability accounts for the reasons why the neural population could be able to coordinate rapidly (Deco and Kringelbach, 2016). Metastability plays a vital role in information-processing, cognitive

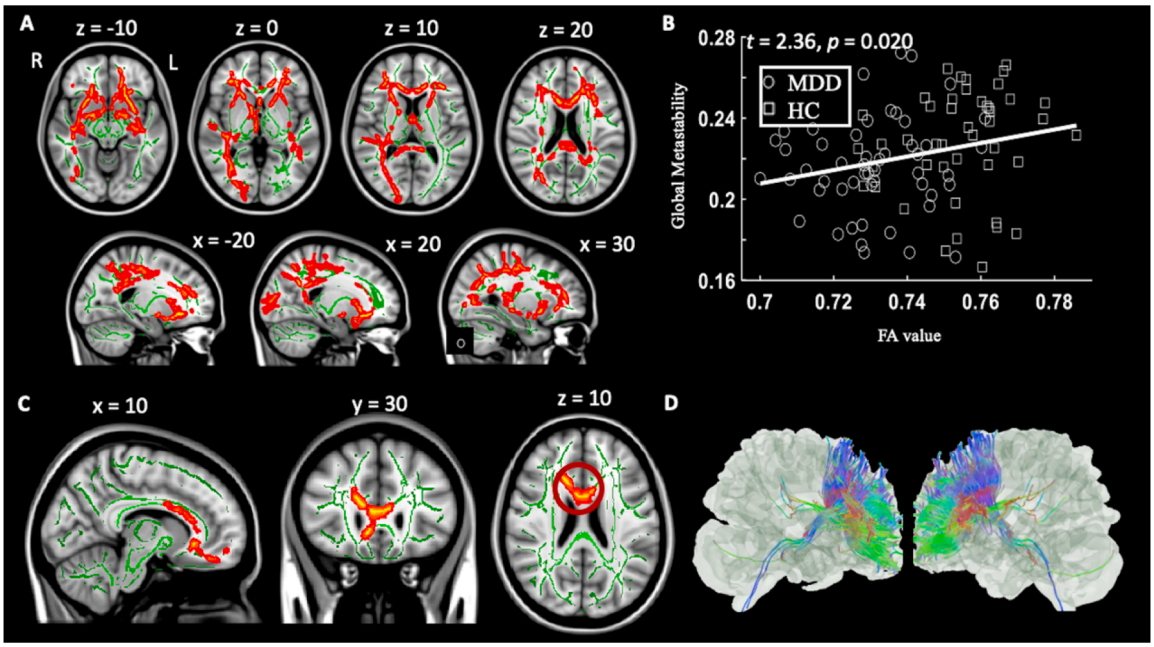

Fig. 4. Alterations in white matter integrity in MDD. (A) Compared to the healthy control group, individuals with major depressive disorder (MDD) showed widespread white matter integrity deficits as indexed by decreased fractional anisotropy (FA; $p < 0.05$, threshold-free cluster enhancement [TFCE] corrected). (B) Average fractional anisotropy (FA) values in white matter integrity deficits were positively correlated with global metastability across all individuals. (C) White matter integrity showing positive relationship with global metastability in individuals with MDD ($p < 0.05$, TFCE corrected). (D) A 3-D illustration of the tracts presented in the genu of the corpus callosum cluster.

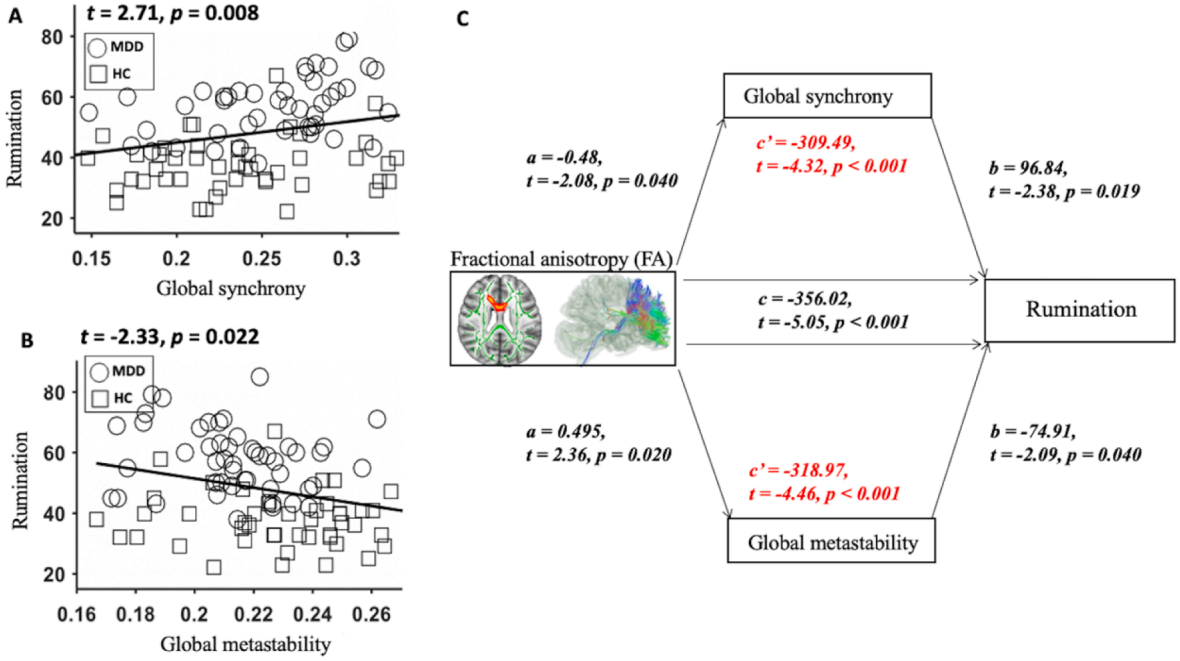

Fig. 5. Dynamic functional connectivity mediated the association between prefrontal white matter integrity and rumination. (A) Global synchrony was positively correlated with total Ruminative Response Scale (RRS) scores. (B) Global metastability was negatively correlated with the total RRS scores. (C) Global synchrony and global metastability respectively mediated the association between prefrontal white matter integrity and rumination.

flexibility, and memory performance (Deco et al., 2009). When metastability is optimal, the neural system can best explore the dynamic repertoire (Kelso, 2012). Kringelbach and Berridge (2017) hypothesized that optimal metastability could be a key factor in emotion and cognition: greater capacity in changing functional configuration in response to rapidly changing external inputs is reflected by higher metastability. During resting-state, individuals with higher metastability exhibit higher information processing speed, better cognitive flexibility, inhibitory control performance, and memory recall (Hellyer et al., 2015; Lee et al., 2019). Contrarily, functional configurations over longer time scales are maintained by lower metastability (Kringelbach and Berridge, 2017). This is in line with the function of lower metastability when it comes to supporting sustained mental operations (Lee et al., 2019; Power et al., 2011; Smith et al., 2009). Indeed, we illustrated that

depressed and ruminative individuals have lower metastability. As rumination is an internal affective-cognitive state featured by repeated thinking of current self-distress and past negative events (Smith and Alloy, 2009), the increased global synchronization with decreased metastability observed suggest that under a task-free state (i.e., resting state), these individuals may linger in a state where the overall phase coupling among areas is persistently high (Lee et al., 2019; Power et al., 2011; Smith et al., 2009), and consequently, fail to transit to other brain states flexibly, plunging deeper into a rumination cycle. Functionally speaking, ruminators are more prone to experiencing further attentional narrowing to self-related information than other-related information (Grol et al., 2015). Individuals possessing a narrow attention scope will thus hold a restricted range of information in their working memory, experience greater difficulty inhibiting or disengaging from specific information, and lack flexibility to switch to new information (Gable and Harmon-Jones, 2012). The aforementioned illuminates the process through which abnormal dynamic connectivity characterizes and perpetuates rumination (Davis and Nolen-Hoeksema, 2000; Joormann et al., 2007; Watkins and Brown, 2002). If exacerbated, repetitive negative thinking may also prolong and exacerbate depressive episodes, increasing the risk for subsequent development of episodes among mood disorders (Nolen-Hoeksema et al., 2008).

To further explain the relationship between decreased metastability and rumination, we speculated that the difficulty with transitioning between brain states may be a reinforcer of rumination and the culprit of the inability to experience hedonic happiness. A factor affecting the subjective feeling of happiness is rumination (Eldeleklioğlu, 2015; Elliott and Coker, 2008). Kringelbach and Berridge (2017) hypothesized that optimal metastability could be a critical element in perceived eudaimonia (the life well-lived) and wellbeing. Under this framework, a possible correspondence could exist between optimal information flow in the pleasure system and the sense of subjective well-being. Rumination could be derived from anhedonia (Grillo, 2016), thereby, decreased metastability may be associated with happiness / pleasure distortions (Addis et al., 2007), with rumination heavily implicated in the relationship but this needs to be further empirically examined.

With the understanding that rumination plays a significant role in the pathology of mood disorders by perpetuating self-focus, negative stressors, and negative affect (Moberly and Watkins, 2008; Watkins, 2008), the association between dynamic functional connectivity and rumination may offer more insights into why lingering in a ruminative state could contribute to worsening affective and cognitive deficits (Demeyer et al., 2012; Joormann et al., 2007; Watkins and Brown, 2002). This, therefore, corroborates that metastability provides a new outlook to understand the brain dynamic processes for psychopathological behaviors (Kringelbach et al., 2015).

5.2. *Prefrontal white matter integrity deficits are associated with rumination*

Networks of anatomical connections are the foundation of dynamic functional connectivity because structural connectivity provides a scaffold for functional connectivity (Avena-Koenigsberger et al., 2018; Deco et al., 2011; Hellyer et al., 2014; Honey et al., 2010; Kelso, 2012). We found that lower metastability was accompanied by widespread alterations of structural connectivity as implied by deficits in white matter integrity, and these deficits were consistent with existing findings (Guo et al., 2012; Korgaonkar et al., 2011; Liao et al., 2013). In alignment with our expectation, the largest alterations were found in the genu of the corpus callosum interconnecting bilateral prefrontal regions, consistent with previous evidence that specific structural correlates could reflect individual differences in rumination (Joormann et al., 2007; Vanderhasselt et al., 2011). The corpus callosum is the largest fiber bundle connecting the left and right hemispheres which serves to integrate cognitive and behavioral functions by enabling the transfer of information between hemispheres, and plays a significant role in motor, perceptual, cognitive, and affective functions (Bloom and Hynd, 2005; Myers, 1956; Wahl et al., 2007). Abnormal reduction in white matter volume of the corpus callosum is evident in mood disorders (Price and Drevets, 2012), with altered structural integrity in the mood regulating circuit correlated with the severity of rumination (Clark et al., 2009; Sexton et al., 2009; Zuo et al., 2012). More white matter integrity is reflected by higher fractional anisotropy (FA), and is associated with better attention control and suppression of irrelevant information, whereas, lower FA values in the genu of the corpus callosum is associated with higher interference and impaired inhibition performance (Rizk et al., 2017). Therefore, the differences in rumination observed in our sample may be explained by integrity differences in the corpora callosa. Ruminators may have greater impairment of cognitive inhibition and an inability to ignore negative thoughts, this could result in the excessive and repetitive rehearsal of their perceived negativity.

5.3. *Aberrant metastability mediates the association between prefrontal white matter integrity and rumination*

We demonstrated that metastability mediated the association between structural integrity of the genu of the corpus callosum and rumination. This serves as preliminary evidence for white matter integrity as a structural basis in the relationship between the repertoire of brain dynamics and rumination. Fibers passing through the genu of the corpus callosum bypass areas including the bilateral prefrontal and orbitofrontal cortices. These areas are viewed as essential for decision-making, executive function, reward processing, and emotional regulation (Mooshagian, 2008; Wahl et al., 2007). The corpus callosum forms the largest myelinated inter-hemispheric structure (Kieseppä et al., 2010), and white matter integrity deficits generally originate from myelin or axonal damage (Jones et al., 2013). Demyelination in the genu of the corpus callosum leads to a decrease in speed or quantity of inter-hemispheric connections (Schulte and Müller-Oehring, 2010; van der Knaap and van der Ham, 2011; R. Zhang et al., 2016), which may manifest as altered temporal dynamics of the inter-hemispheric functional connectivity. Past studies have demonstrated the dynamic nature of inter-hemispheric communications over time (Doron et al., 2012), and this was speculated to be associated with connections through the corpus callosum (Sperry et al., 1969), wherein its white matter integrity is of paramount importance for cognitive inhibition, a key mechanism that underlies emotional regulation, the suppression of irrelevant negative information, and rumination (Demeyer et al., 2012; Joormann, 2010).

The focus of this study is on dynamic functional connectivity, but findings from clinical studies have also suggested that structural damage to the corpus callosum are connected with alterations in the prefrontal, parietal, and limbic regions (Sharp et al., 2011), regions that are largely related to the default mode network (DMN). The DMN serves internally focused processes, and is significantly involved in the task-free state, mind-wandering, and self-referential processing (Raichle, 2015). Such an observation may be accounted for by the topographical organization of the corpus callosum where its shape could lead to differential effects on functionally connected brain areas (Walterfang et al., 2009). Therefore, prefrontal white matter integrity deficits observed in our ruminators could be related to significant dominance of the DMN, which results in impaired representations of the self and internal modes of cognition (Buckner et al., 2008), as well as decreased hedonic well-being (Luo et al., 2016), cuing high levels of automatic and maladaptive rumination (Hamilton et al., 2015; Hamilton et al., 2011). Our findings suggested a potential neural mechanism where disruptions to the callosal structure could lead to widespread disturbances to connectivity related to functional impairments in the mood regulating path, triggering stronger neural activity in related networks during rumination, such as the DMN (Cooney et al., 2010). Therefore, we proposed that structural alterations in the corpus callosum could be a major biological change in the phenomenon of rumination. Prospective studies are recommended to

examine this further in connection with DMN and other related networks. Our findings aligned with previous interpretations that structural connectivity can restrict the dynamicity of functional connectivity in the brain (Liégeois et al., 2016; Park et al., 2017). Hence, investigating structural integrity in white matter in addition to the brain dynamical repertoire would offer a more integrative understanding on the neural basis of rumination.

It is also important to note that although we have presented findings suggesting that (ab)normal transitions between brain states plays an essential role in the connection of structural connectivity in ruminative thinking, the presence of a causal relationship between metastability and rumination could not be determined at the current stage and we must await future research to further validate our results. Future studies could consider employing non-invasive brain stimulation techniques, such as transcranial magnetic stimulation (TMS) and transcranial direct current stimulation (tDCS) to establish causality, i.e., whether brain stimulation can affect global metastability, and correspondingly the severity of rumination via changes in neural mechanisms. Reassuringly, studies have found success with brain stimulation when it comes to improving brain and behavioral functional outcomes (Kunze et al., 2016; Shang et al., 2020; Steel et al., 2016; Yu et al., 2015), suggesting that improving metastability and rumination with brain stimulation could be a promising endeavor.

5.4. Limitations

This study is not without limitations. Firstly, for ethical reasons, our MDD sample was on antidepressant medication. Antidepressants normalize network functional connectivity (Goldstein-Piekarski et al., 2018; Posner et al., 2013), which could pose potential medication confounds. Moreover, the MDD individuals experienced different depressive episodes and episode duration which made it difficult to ascertain whether neural abnormalities relating to rumination were present prior to illness onset, thereby, representing a putative vulnerability factor. Nevertheless, other potential confounding factors should be minimized as we only recruited participants who were on stable medications and did not receive electroconvulsive therapy within a six-month period before data collection. However, we encourage future studies to recruit only first-episode, treatment-naïve, and medication-free samples to target more closely the neural underpinnings of rumination.

Secondly, it is important to consider the multi-component nature of rumination (Raes et al., 2008). Although we utilized the RRS which measures three ruminative subcomponents, rumination is a complex regime involving affective and cognitive subprocesses (Cooney et al., 2010), and could be accompanied by maladaptive and adaptive behaviors (Joormann et al., 2006). Hence, rumination could be a multifactorial set of processes not only limited to depression, brooding, and reflection. With this in mind, readers ought to interpret our findings with caution as there could be ruminative subcomponents yet to be explored.

Thirdly, admittedly, we adopted a task-free approach which may only offer a narrow perspective on the neural basis of rumination. This is because a ruminative state could be triggered by internal (e.g., negative affect) or external events that conflict with an individual's goals (Koster et al., 2011). Therefore, our findings warrant careful interpretation. That said, studying dynamic functional connectivity in a resting state could shed light on task-related spatiotemporal organization in the brain as under a resting state, maximal metastability would facilitate task-related brain systems configuration (Hellyer et al., 2014), and dysfunctions among different functional systems may reflect core underlying affective and cognitive abnormalities (Kaiser et al., 2015). In light of this, it was our intention to investigate the role of dynamic connectivity in mediating the association between structural connectivity and rumination before the introduction of manipulations, e.g., tasks inducing rumination / measuring affective interference / cognitive inhibition, and brain stimulation techniques into the study.

6. Conclusions

This study offered a new perspective to understand the aberrant dynamic functional connectivity associated with structural connectivity and rumination. Specifically, global metastability and global synchrony forms the basis of the association between connectivity in the genu of the corpus callosum to rumination, wherein dynamic connectivity is heavily involved in cognitive control and the suppression of irrelevant negative information. Our findings provided a framework where optimal functional metastability may be essential for disengaging attention from a ruminative state, and presented the first line of evidence for the important mediating role abnormal transitions between brain states may play in the white matter integrity deficits in ruminative thinking.

Funding

This work was supported by the Key-Area Research and Development Program of Guangdong Province (2018B30334001) and The University of Hong Kong May Endowed Professorship in Neuropsychology to Tatia Lee; the National Natural Science Foundation of China (NSFC: 31900806) to Ruibin Zhang; and the Science and Technology Program of Guangzhou, China, No. 202007030012 to Kangguang Lin.

Author contributions

Ruibin Zhang: Methodology, Project administration, Data curation, Formal analysis, Investigation, Writing – original draft, Funding acquisition. **Sammi-Kenzie T.S. Tam:** Writing – original draft. Nichol M.L. Wong: Investigation, Writing – review & editing. **Jingsong Wu:** Writing – review & editing. **Jing Tao:** Writing – review & editing. Lidian Chen: Writing – review & editing. **Kangguang Lin:** Project administration, Data curation, Writing – review & editing, Funding acquisition. **Tatia M. C. Lee:** Conceptualization, Methodology, Investigation, Writing – review & editing, Supervision, Funding acquisition.

Declaration of Competing Interest

The authors declare that they have no known competing financial interests or personal relationships that could have appeared to influence the work reported in this paper.

Appendix A. Supplementary data

Supplementary data to this article can be found online at https://doi.org/10.1016/j.nicl.2021.102916.

References

Addis, D.R., Wong, A.T., Schacter, D.L., 2007. Remembering the past and imagining the future: common and distinct neural substrates during event construction and elaboration. Neuropsychologia 45 (7), 1363–1377. https://doi.org/10.1016/j.neuropsychologia.2006.10.016.

Alderson, T.H., Bokde, A.L.W., Kelso, J.A.S., Maguire, L., Coyle, D., 2020. Metastable neural dynamics underlies cognitive performance across multiple behavioural paradigms. Hum. Brain Mapp. 41 (12), 3212–3234. https://doi.org/10.1002/hbm.v41.1210.1002/hbm.25009.

Avena-Koenigsberger, A., Misic, B., Sporns, O., 2018. Communication dynamics in complex brain networks. Nat. Rev. Neurosci. 19 (1), 17–33. https://doi.org/10.1038/nrn.2017.149.

Bi, Y., He, Y., 2014. Connectomics reveals faulty wiring patterns for depressed brain. Biol. Psychiatry 76 (7), 515–516. https://doi.org/10.1016/j.biopsych.2014.07.002.

Bloom, J.S., Hynd, G.W., 2005. The role of the corpus callosum in interhemispheric transfer of information: excitation or inhibition? Neuropsychol. Rev. 15 (2), 59–71. https://doi.org/10.1007/s11065-005-6252-y.

Borchers L.R., Bruckert L., Mastrovito D., King L.S., Ho T.C., Gotlib I.H., 2019. Rumination mediates associations between white matter microstructure of the cerebellar peduncles and depression in adolescence. doi.org/10.13140/RG.2.2.19259.26408.

Buckner, R.L., Andrews-Hanna, J.R., Schacter, D.L., 2008. The brain's default network: anatomy, function, and relevance to disease. In: The Year in Cognitive Neuroscience

2008. Annals of the New York Academy of Sciences. Blackwell Publishing, Malden, pp. 1–38.
Cabral, J., Hugues, E., Sporns, O., Deco, G., 2011. Role of local network oscillations in resting-state functional connectivity. NeuroImage 57 (1), 130–139. https://doi.org/10.1016/j.neuroimage.2011.04.010.
Calhoun, V.D., Adali, T., Pearlson, G.D., Pekar, J.J., 2001. A method for making group inferences from functional MRI data using independent component analysis. Hum. Brain Mapp. 14 (3), 140–151. https://doi.org/10.1002/(ISSN)1097-019310.1002/hbm.v14:310.1002/hbm.1048.
Calhoun, V., Miller, R., Pearlson, G., Adalı, T., 2014. The Chronnectome: time-Varying Connectivity Networks as the Next Frontier in fMRI Data Discovery. Neuron 84 (2), 262–274. https://doi.org/10.1016/j.neuron.2014.10.015.
Chen, G., Chen, G., Xie, C., Ward, B.D., Li, W., Antuono, P., Li, S.-J., 2012. A method to determine the necessity for global signal regression in resting-state fMRI studies. Magn. Reson. Med. 68 (6), 1828–1835. https://doi.org/10.1002/mrm.v68.610.1002/mrm.24201.
Clark, L., Chamberlain, S.R., Sahakian, B.J., 2009. Neurocognitive mechanisms in depression: implications for treatment. Annu Rev Neurosci 32 (1), 57–74.
Cooney, R.E., Joormann, J., Eugène, F., Dennis, E.L., Gotlib, I.H., 2010. Neural correlates of rumination in depression. Cogn. Affect. Behav. Neurosci. 10 (4), 470–478. https://doi.org/10.3758/CABN.10.4.470.
Cusin, C., Yang, H., Yeung, A., Fava, M., 2009. Rating Scales for depression. In: Handbook of clinical rating scales and assessment in psychiatry and mental health. Humana Press, pp. 7–35. https://doi.org/10.1007/978-1-59745-387-5_2.
Davis, R.N., Nolen-Hoeksema, S., 2000. Cognitive inflexibility among ruminators and nonruminators. Cogn. Ther. Res. 24, 699–711. https://doi.org/10.1023/A:1005591412406.
Deco, G., Jirsa, V., McIntosh, A.R., Sporns, O., Kotter, R., 2009. Key role of coupling, delay, and noise in resting brain fluctuations. Proc. Natl. Acad. Sci. 106 (25), 10302–10307. https://doi.org/10.1073/pnas.0901831106.
de Schotten, M.T., Foulon, C., Nachev, P., 2020. Brain disconnections link structural connectivity with function and behaviour. Nat. Commun. 11, 5094. https://doi.org/10.1038/s41467-020-18920-9.
Deco, G., Jirsa, V.K., McIntosh, A.R., 2011. Emerging concepts for the dynamical organization of resting-state activity in the brain. Nat. Rev. Neurosci. 12 (1), 43–56. https://doi.org/10.1038/nrn2961.
Deco, G., Kringelbach, M.L., 2016. Metastability and coherence: extending the communication through coherence hypothesis using a whole-brain computational perspective. Trends Neurosci. 39 (3), 125–135. https://doi.org/10.1016/j.tins.2016.01.001.
Demeyer, I., De Lissnyder, E., Koster, E.H.W., De Raedt, R., 2012. Rumination mediates the relationship between impaired cognitive control for emotional information and depressive symptoms: a prospective study in remitted depressed adults. Behav. Res. Ther. 50 (5), 292–297. https://doi.org/10.1016/j.brat.2012.02.012.
Demirtaş, M., Tornador, C., Falcón, C., López-Solà, M., Hernández-Ribas, R., Pujol, J., Menchón, J.M., Ritter, P., Cardoner, N., Soriano-Mas, C., Deco, G., 2016. Dynamic functional connectivity reveals altered variability in functional connectivity among patients with major depressive disorder. Hum. Brain Mapp. 37 (8), 2918–2930. https://doi.org/10.1002/hbm.v37.810.1002/hbm.23215.
Doron, K.W., Bassett, D.S., Gazzaniga, M.S., 2012. Dynamic network structure of interhemispheric coordination. Proc. Natl. Acad. Sci. 109 (46), 18661–18668. https://doi.org/10.1073/pnas.1216402109.
Eldeleklioğlu, J., 2015. Predictive effects of subjective happiness, forgiveness, and rumination on life satisfaction. Soc. Behav. Personal. Int. J. 43 (9), 1563–1574. https://doi.org/10.2224/sbp.2015.43.9.1563.
Elliott, I., Coker, S., 2008. Independent self-construal, self-reflection, and self-rumination: a path model for predicting happiness. Aust. J. Psychol. 60 (3), 127–134. https://doi.org/10.1080/00049530701447368.
Ferreira, L.N., Zhao, L., 2016. Time series clustering via community detection in networks. Inf. Sci. 326, 227–242. https://doi.org/10.1016/j.ins.2015.07.046.
Fox, M.D., Raichle, M.E., 2007. Spontaneous fluctuations in brain activity observed with functional magnetic resonance imaging. Nat. Rev. Neurosci. 8 (9), 700–711. https://doi.org/10.1038/nrn2201.
Fries, P., 2015. Rhythms for cognition: communication through coherence. Neuron 88 (1), 220–235. https://doi.org/10.1016/j.neuron.2015.09.034.
Gable, P.A., Harmon-Jones, E., 2012. Reducing attentional capture of emotion by broadening attention: increased global attention reduces early electrophysiological responses to negative stimuli. Biol. Psychol. 90 (2), 150–153. https://doi.org/10.1016/j.biopsycho.2012.02.006.
Glerean, E., Salmi, J., Lahnakoski, J.M., Jääskeläinen, I.P., Sams, M., 2012. Functional magnetic resonance imaging phase synchronization as a measure of dynamic functional connectivity. Brain Connect. 2 (2), 91–101. https://doi.org/10.1089/brain.2011.0068.
Goldstein-Piekarski, A.N., Staveland, B.R., Ball, T.M., Yesavage, J., Korgaonkar, M.S., Williams, L.M., 2018. Intrinsic functional connectivity predicts remission on antidepressants: a randomized controlled trial to identify clinically applicable imaging biomarkers. Transl. Psychiatry 8, 1–11. https://doi.org/10.1038/s41398-018-0100-3.
Gong, Q., He, Y., 2015. Depression, neuroimaging and connectomics: a selective overview. Biol. Psychiatry, The Development and Progression of Depression 77 (3), 223–235. https://doi.org/10.1016/j.biopsych.2014.08.009.
Grillo, L., 2016. A possible role of anhedonia as common substrate for depression and anxiety. Depress. Res. Treat. 2016, 1–8. https://doi.org/10.1155/2016/1598130.
Grol, M., Hertel, P.T., Koster, E.H.W., De Raedt, R., 2015. The effects of rumination induction on attentional breadth for self-related information. Clin. Psychol. Sci. 3 (4), 607–618. https://doi.org/10.1177/2167702614566814.
Guo, W.-B., Liu, F., Chen, J.-D., Xu, X.-J., Wu, R.-R., Ma, C.-Q., Gao, K., Tan, C.-L., Sun, X.-l., Xiao, C.-Q., Chen, H.-f., Zhao, J.-P., 2012. Altered white matter integrity of forebrain in treatment-resistant depression: a diffusion tensor imaging study with tract-based spatial statistics. Prog. Neuropsychopharmacol. Biol. Psychiatry 38 (2), 201–206. https://doi.org/10.1016/j.pnpbp.2012.03.012.
Hamilton, M., 1986. The Hamilton Rating Scale for Depression. In: Sartorius, N., Ban, T. A. (Eds.), Assessment of Depression. Springer, Berlin, Heidelberg, pp. 143–152. https://doi.org/10.1007/978-3-642-70486-4_14.
Hamilton, J.P., Farmer, M., Fogelman, P., Gotlib, I.H., 2015. Depressive rumination, the default-mode network, and the dark matter of clinical neuroscience. Biol. Psychiatry, Depression 78 (4), 224–230. https://doi.org/10.1016/j.biopsych.2015.02.020.
Hamilton, J.P., Furman, D.J., Chang, C., Thomason, M.E., Dennis, E., Gotlib, I.H., 2011. Default-mode and task-positive network activity in major depressive disorder: implications for adaptive and maladaptive rumination. Biol. Psychiatry 70 (4), 327–333. https://doi.org/10.1016/j.biopsych.2011.02.003.
Han, X., Yang, H., 2009. Chinese version of Nolen-Hoeksema Ruminative Responses Scale (RRS) used in 912 college students: reliability and validity. Chin. J. Clin. Psychol. 17, 550–551.
Hansen, E.C.A., Battaglia, D., Spiegler, A., Deco, G., Jirsa, V.K., 2015. Functional connectivity dynamics: modeling the switching behavior of the resting state. NeuroImage 105, 525–535. https://doi.org/10.1016/j.neuroimage.2014.11.001.
Harrington, D.L., Rubinov, M., Durgerian, S., Mourany, L., Reece, C., Koenig, K., Bullmore, E.d., Long, J.D., Paulsen, J.S., Rao, S.M., 2015. Network topology and functional connectivity disturbances precede the onset of Huntington's disease. Brain 138 (8), 2332–2346. https://doi.org/10.1093/brain/awv145.
Hellyer, P.J., Scott, G., Shanahan, M., Sharp, D.J., Leech, R., 2015. Cognitive flexibility through metastable neural dynamics is disrupted by damage to the structural connectome. J. Neurosci. Off. J. Soc. Neurosci. 35 (24), 9050–9063. https://doi.org/10.1523/JNEUROSCI.4648-14.2015.
Hellyer, P.J., Shanahan, M., Scott, G., Wise, R.J.S., Sharp, D.J., Leech, R., 2014. The control of global brain dynamics: opposing actions of frontoparietal control and default mode networks on attention. J. Neurosci. 34 (2), 451–461. https://doi.org/10.1523/JNEUROSCI.1853-13.2014.
Himberg, J., Hyvärinen, A., Esposito, F., 2004. Validating the independent components of neuroimaging time series via clustering and visualization. NeuroImage 22 (3), 1214–1222. https://doi.org/10.1016/j.neuroimage.2004.03.027.
Honey, C.J., Thivierge, J.-P., Sporns, O., 2010. Can structure predict function in the human brain? NeuroImage 52 (3), 766–776. https://doi.org/10.1016/j.neuroimage.2010.01.071.
Jones, D.K., Knösche, T.R., Turner, R., 2013. White matter integrity, fiber count, and other fallacies: the do's and don'ts of diffusion MRI. NeuroImage 73, 239–254. https://doi.org/10.1016/j.neuroimage.2012.06.081.
Joormann, J., 2010. Cognitive inhibition and emotion regulation in depression. Curr. Dir. Psychol. Sci. 19 (3), 161–166. https://doi.org/10.1177/0963721410370293.
Joormann, J., Dkane, M., Gotlib, I.H., 2006. Adaptive and maladaptive components of rumination? Diagnostic specificity and relation to depressive biases. Behav. Ther. 37 (3), 269–280. https://doi.org/10.1016/j.beth.2006.01.002.
Joormann, J., Yoon, K.L., Zetsche, U., 2007. Cognitive inhibition in depression. Appl. Prev. Psychol. 12 (3), 128–139. https://doi.org/10.1016/j.appsy.2007.09.002.
Kaiser, R.H., Andrews-Hanna, J.R., Wager, T.D., Pizzagalli, D.A., 2015. Large-scale network dysfunction in major depressive disorder: a meta-analysis of resting-state functional connectivity. JAMA Psychiatry 72, 603–611. https://doi.org/10.1001/jamapsychiatry.2015.0071.
Kaiser, R.H., Whitfield-Gabrieli, S., Dillon, D.G., Goer, F., Beltzer, M., Minkel, J., Smoski, M., Dichter, G., Pizzagalli, D.A., 2016. Dynamic resting-state functional connectivity in major depression. Neuropsychopharmacology 41 (7), 1822–1830. https://doi.org/10.1038/npp.2015.352.
Kelly, R.E., Alexopoulos, G.S., Wang, Z., Gunning, F.M., Murphy, C.F., Morimoto, S.S., Kanellopoulos, D., Jia, Z., Lim, K.O., Hoptman, M.J., 2010. Visual inspection of independent components: defining a procedure for artifact removal from fMRI data. J. Neurosci. Methods 189 (2), 233–245. https://doi.org/10.1016/j.jneumeth.2010.03.028.
Kelso, J.A.S., 2012. Multistability and metastability: understanding dynamic coordination in the brain. Philos. Trans. R. Soc. B Biol. Sci. 367 (1591), 906–918. https://doi.org/10.1098/rstb.2011.0351.
Kieseppä, T., Eerola, M., Mäntylä, R., Neuvonen, T., Poutanen, V.-P., Luoma, K., Tuulio-Henriksson, A., Jylhä, P., Mantere, O., Melartin, T., Rytsälä, H., Vuorilehto, M., Isometsä, E., 2010. Major depressive disorder and white matter abnormalities: a diffusion tensor imaging study with tract-based spatial statistics. J. Affect. Disord. 120, 240–244. https://doi.org/10.1016/j.jad.2009.04.023.
Korgaonkar, M.S., Grieve, S.M., Koslow, S.H., Gabrieli, J.D.E., Gordon, E., Williams, L. M., 2011. Loss of white matter integrity in major depressive disorder: evidence using tract-based spatial statistical analysis of diffusion tensor imaging. Hum. Brain Mapp. 32 (12), 2161–2171. https://doi.org/10.1002/hbm.v32.1210.1002/hbm.21178.
Koster, E.H.W., De Lissnyder, E., Derakshan, N., De Raedt, R., 2011. Understanding depressive rumination from a cognitive science perspective: the impaired disengagement hypothesis. Clin. Psychol. Rev. 31 (1), 138–145. https://doi.org/10.1016/j.cpr.2010.08.005.
Kovács, L.N., Takacs, Z.K., Tóth, Z., Simon, E., Schmelowszky, Á., Kökönyei, G., 2020. Rumination in major depressive and bipolar disorder – a meta-analysis. J. Affect. Disord. 276, 1131–1141. https://doi.org/10.1016/j.jad.2020.07.131.
Kringelbach, M.L., Berridge, K.C., 2017. The affective core of emotion: linking pleasure, subjective well-being, and optimal metastability in the brain. Emot. Rev. 9 (3), 191–199. https://doi.org/10.1177/1754073916684558.

Kringelbach, M.L., McIntosh, A.R., Ritter, P., Jirsa, V.K., Deco, G., 2015. The rediscovery of slowness: exploring the timing of cognition. Trends Cogn. Sci. 19 (10), 616–628. https://doi.org/10.1016/j.tics.2015.07.011.

Kunze, T., Hunold, A., Haueisen, J., Jirsa, V., Spiegler, A., 2016. Transcranial direct current stimulation changes resting state functional connectivity: a large-scale brain network modeling study. NeuroImage, Transcranial electric stimulation (tES) and Neuroimaging 140, 174–187. https://doi.org/10.1016/j.neuroimage.2016.02.015.

Lachaux, J.-P., Rodriguez, E., Martinerie, J., Varela, F.J., 1999. Measuring phase synchrony in brain signals. Hum. Brain Mapp. 8, 194–208. https://doi.org/10.1002/(SICI)1097-0193(1999)8:4<194::AID-HBM4>3.0.CO;2-C.

Lee, W.H., Moser, D.A., Ing, A., Doucet, G.E., Frangou, S., 2019. Behavioral and health correlates of resting-state metastability in the human connectome project. Brain Topogr. 32 (1), 80–86. https://doi.org/10.1007/s10548-018-0672-5.

Liao, Y., Huang, X., Wu, Q., Yang, C., Kuang, W., Du, M., Lui, S, Yue, Q., Chan, R.C.K., Kemp, G.J., Gong, Q., 2013. Is depression a disconnection syndrome? Meta-analysis of diffusion tensor imaging studies in patients with MDD. J. Psychiatry Neurosci. 38 (1), 49–56. https://doi.org/10.1503/jpn10.1503/jpn.110180.

Liégeois, R., Ziegler, E., Phillips, C., Geurts, P., Gómez, F., Bahri, M.A., Yeo, B.T.T., Soddu, A., Vanhaudenhuyse, A., Laureys, S., Sepulchre, R., 2016. Cerebral functional connectivity periodically (de)synchronizes with anatomical constraints. Brain Struct. Funct. 221 (6), 2985–2997. https://doi.org/10.1007/s00429-015-1083-y.

Lisy, M.E., Jarvis, K.B., DelBello, M.P., Mills, N.P., Weber, W.A., Fleck, D., Strakowski, S. M., Adler, C.M., 2011. Progressive neurostructural changes in adolescent and adult patients with bipolar disorder. Bipolar Disord. 13, 396–405. https://doi.org/10.1111/j.1399-5618.2011.00927.x.

Liu, J., Liao, X., Xia, M., He, Y., 2018. Chronnectome fingerprinting: identifying individuals and predicting higher cognitive functions using dynamic brain connectivity patterns. Hum. Brain Mapp. 39 (2), 902–915. https://doi.org/10.1002/hbm.v39.210.1002/hbm.23890.

Liu, M., Wang, Y., Zhang, A., Yang, C., Liu, P., Wang, J., Zhang, K., Wang, Y., Sun, N., 2021. Altered dynamic functional connectivity across mood states in bipolar disorder. Brain Res. 1750, 147143. https://doi.org/10.1016/j.brainres.2020.147143.

Lu, Y., Shen, Z., Cheng, Y., Yang, H., He, B., Xie, Y., Wen, L., Zhang, Z., Sun, X., Zhao, W., Xu, X., Han, D., 2017. Alternations of white matter structural networks in first episode untreated major depressive disorder with short duration. Front. Psychiatry 8, 205. https://doi.org/10.3389/fpsyt.2017.00205.

Luo, Y., Kong, F., Qi, S., You, X., Huang, X., 2016. Resting-state functional connectivity of the default mode network associated with happiness. Soc. Cogn. Affect. Neurosci. 11 (3), 516–524. https://doi.org/10.1093/scan/nsv132.

Martínez, S.A., Marsman, J.B.C., Kringelbach, M.L., Deco, G., Ter Horst, G.J., 2020. Reduced spatiotemporal brain dynamics are associated with increased depressive symptoms after a relationship breakup. NeuroImage Clin. 27, 102299. https://doi.org/10.1016/j.nicl.2020.102299.

Moberly, N.J., Watkins, E.R., 2008. Ruminative self-focus, negative life events, and negative affect. Behav. Res. Ther. 46 (9), 1034–1039. https://doi.org/10.1016/j.brat.2008.06.004.

Mooshagian, E., 2008. Anatomy of the corpus callosum reveals its function. J. Neurosci. 28 (7), 1535–1536. https://doi.org/10.1523/JNEUROSCI.5426-07.2008.

Myers, R.E., 1956. Function of corpus callosum in interocular transfer. Brain 79 (2), 358–363. https://doi.org/10.1093/brain/79.2.358.

Nolen-Hoeksema, S., 2000. The role of rumination in depressive disorders and mixed anxiety/depressive symptoms. J. Abnorm. Psychol. 109, 504–511. https://doi.org/10.1037/0021-843X.109.3.504.

Nolen-Hoeksema, S., Wisco, B.E., Lyubomirsky, S., 2008. Rethinking rumination. Perspect. Psychol. Sci. 3 (5), 400–424. https://doi.org/10.1111/j.1745-6924.2008.00088.x.

Pajevic, S., Basser, P.J., Fields, R.D., 2014. Role of myelin plasticity in oscillations and synchrony of neuronal activity. Neuroscience 276, 135–147. https://doi.org/10.1016/j.neuroscience.2013.11.007.

Papageorgiou, C., Siegle, G.J., 2003. Rumination and depression: advances in theory and research. Cogn. Ther. Res. 27, 243–245. https://doi.org/10.1023/A:1023918331490.

Park, B., Eo, J., Park, H.-J., 2017. Structural brain connectivity constrains within-a-day variability of direct functional connectivity. Front. Hum. Neurosci. 11, 408. https://doi.org/10.3389/fnhum.2017.00408.

Park, H.-J., Friston, K.J., Pae, C., Park, B., Razi, A., 2018. Dynamic effective connectivity in resting state fMRI. NeuroImage 180, 594–608. https://doi.org/10.1016/j.neuroimage.2017.11.033.

Pedersen, M., Omidvarnia, A., Zalesky, A., Jackson, G.D., 2018a. On the relationship between instantaneous phase synchrony and correlation-based sliding windows for time-resolved fMRI connectivity analysis. NeuroImage 181, 85–94. https://doi.org/10.1016/j.neuroimage.2018.06.020.

Pedersen, M., Zalesky, A., Omidvarnia, A., Jackson, G.D., 2018b. Multilayer network switching rate predicts brain performance. Proc. Natl. Acad. Sci. 115 (52), 13376–13381. https://doi.org/10.1073/pnas.1814785115.

Penke, L., Maniega, S.M., Bastin, M.E., Valdés Hernández, M.C., Murray, C., Royle, N.A., Starr, J.M., Wardlaw, J.M., Deary, I.J., 2012. Brain white matter tract integrity as a neural foundation for general intelligence. Mol. Psychiatry 17 (10), 1026–1030. https://doi.org/10.1038/mp.2012.66.

Pisner, D.A., Shumake, J., Beevers, C.G., Schnyer, D.M., 2018. A reproducible neurobiology of depressive rumination. bioRxiv 365759. https://doi.org/10.1101/365759.

Ponce-Alvarez, A., Deco, G., Hagmann, P., Romani, G.L., Mantini, D., Corbetta, M., Hilgetag, C.C., 2015. Resting-state temporal synchronization networks emerge from connectivity topology and heterogeneity. PLOS Comput. Biol. 11 (2), e1004100. https://doi.org/10.1371/journal.pcbi.1004100.

Posner, J., Hellerstein, D.J., Gat, I., Mechling, A., Klahr, K., Wang, Z., McGrath, P.J., Stewart, J.W., Peterson, B.S., 2013. Antidepressants normalize the default mode network in patients with dysthymia. JAMA Psychiatry 70, 373–382. https://doi.org/10.1001/jamapsychiatry.2013.455.

Power, J.D., Barnes, K.A., Snyder, A.Z., Schlaggar, B.L., Petersen, S.E., 2012. Spurious but systematic correlations in functional connectivity MRI networks arise from subject motion. NeuroImage 59 (3), 2142–2154. https://doi.org/10.1016/j.neuroimage.2011.10.018.

Power, J., Cohen, A., Nelson, S., Wig, G., Barnes, K., Church, J., Vogel, A., Laumann, T., Miezin, F., Schlaggar, B., Petersen, S., 2011. Functional network organization of the human brain. Neuron 72 (4), 665–678. https://doi.org/10.1016/j.neuron.2011.09.006.

Price, J.L., Drevets, W.C., 2012. Neural circuits underlying the pathophysiology of mood disorders. Trends Cogn. Sci. 16 (1), 61–71. https://doi.org/10.1016/j.tics.2011.12.011.

Prichard, D., Theiler, J., 1994. Generating surrogate data for time series with several simultaneously measured variables. Phys. Rev. Lett. 73 (7), 951–954. https://doi.org/10.1103/PhysRevLett.73.951.

Rabinovich, M.I., Afraimovich, V.S., Bick, C., Varona, P., 2012. Information flow dynamics in the brain. Phys. Life Rev. 9 (1), 51–73. https://doi.org/10.1016/j.plrev.2011.11.002.

Raes, F., Hermans, D., Williams, J.M.G., Bijttebier, P., Eelen, P., 2008. A "triple W"-model of rumination on sadness: why am I feeling sad, what's the meaning of my sadness, and wish I could stop thinking about my sadness (but I can't!). Cogn. Ther. Res. 32 (4), 526–541. https://doi.org/10.1007/s10608-007-9137-y.

Raichle, M.E., 2015. The brain's default mode network. Annu. Rev. Neurosci. 38 (1), 433–447. https://doi.org/10.1146/neuro.2015.38.issue-110.1146/annurev-neuro-071013-014030.

Rizk, M.M., Rubin-Falcone, H., Keilp, J., Miller, J.M., Sublette, M.E., Burke, A., Oquendo, M.A., Kamal, A.M., Abdelhameed, M.A., Mann, J.J., 2017. White matter correlates of impaired attention control in major depressive disorder and healthy volunteers. J. Affect. Disord. 222, 103–111. https://doi.org/10.1016/j.jad.2017.06.066.

Rosenbaum, D., Haipt, A., Fuhr, K., Haeussinger, F.B., Metzger, F.G., Nuerk, H.-C., Fallgatter, A.J., Batra, A., Ehlis, A.-C., 2017. Aberrant functional connectivity in depression as an index of state and trait rumination. Sci. Rep. 7, 2174. https://doi.org/10.1038/s41598-017-02277-z.

Satterthwaite, T.D., Wolf, D.H., Erus, G., Ruparel, K., Elliott, M.A., Gennatas, E.D., Hopson, R., Jackson, C., Prabhakaran, K., Bilker, W.B., Calkins, M.E., Loughead, J., Smith, A., Roalf, D.R., Hakonarson, H., Verma, R., Davatzikos, C., Gur, R.C., Gur, R. E., 2013. Functional maturation of the executive system during adolescence. J. Neurosci. 33 (41), 16249–16261. https://doi.org/10.1523/JNEUROSCI.2345-13.2013.

Schulte, T., Müller-Oehring, E.M., 2010. Contribution of callosal connections to the interhemispheric integration of visuomotor and cognitive processes. Neuropsychol. Rev. 20 (2), 174–190. https://doi.org/10.1007/s11065-010-9130-1.

Sexton, C.E., Mackay, C.E., Ebmeier, K.P., 2009. A systematic review of diffusion tensor imaging studies in affective disorders. Biol. Psychiatry, Epigenetics and Suicide 66 (9), 814–823. https://doi.org/10.1016/j.biopsych.2009.05.024.

Shang, Y., Chang, D.a., Zhang, J., Peng, W., Song, D., Gao, X., Wang, Z.e., 2020. Theta-burst transcranial magnetic stimulation induced functional connectivity changes between dorsolateral prefrontal cortex and default-mode-network. Brain Imaging Behav. 14 (5), 1955–1963. https://doi.org/10.1007/s11682-019-00139-y.

Sharp, D.J., Beckmann, C.F., Greenwood, R., Kinnunen, K.M., Bonnelle, V., De Boissezon, X., Powell, J.H., Counsell, S.J., Patel, M.C., Leech, R., 2011. Default mode network functional and structural connectivity after traumatic brain injury. Brain 134, 2233–2247. https://doi.org/10.1093/brain/awr175.

Sie, J.-H., Chen, Y.-H., Shiau, Y.-H., Chu, W.-C., 2019. Gender- and age-specific differences in resting-state functional connectivity of the central autonomic network in adulthood. Front. Hum. Neurosci. 13, 369. https://doi.org/10.3389/fnhum.2019.00369.

Smith, J.M., Alloy, L.B., 2009. A roadmap to rumination: a review of the definition, assessment, and conceptualization of this multifaceted construct. Clin. Psychol. Rev. 29 (2), 116–128. https://doi.org/10.1016/j.cpr.2008.10.003.

Smith, S., Jenkinson, M., Woolrich, M., Beckmann, C., Behrens, T., Johansen-Berg, H., Bannister, P., Luca, M., Drobnjak, I., Flitney, D., Niazy, R., Saunders, J., Vickers, J., Zhang, Y., De Stefano, N., Brady, M., Matthews, P., 2004. Advances in functional and structural MR image analysis and implementation as FSL. NeuroImage 23 (Suppl 1), S208–S219. https://doi.org/10.1016/j.neuroimage.2004.07.051.

Smith, S.M., Fox, P.T., Miller, K.L., Glahn, D.C., Fox, P.M., Mackay, C.E., Filippini, N., Watkins, K.E., Toro, R., Laird, A.R., Beckmann, C.F., 2009. Correspondence of the brain's functional architecture during activation and rest. Proc. Natl. Acad. Sci. 106 (31), 13040–13045. https://doi.org/10.1073/pnas.0905267106.

Sperry, R.W., Gazzaniga, M.S., Bogen, J.E., 1969. Interhemispheric relationships: the neocortical commissures; syndromes of hemisphere disconnection. In: Vinken, P., Bruyn, G. (Eds.), Handbook of Clinical Neurology. North Holland, pp. 4–273.

Steel, A., Song, S., Bageac, D., Knutson, K.M., Keisler, A., Saad, Z.S., Gotts, S.J., Wassermann, E.M., Wilkinson, L., 2016. Shifts in connectivity during procedural learning after motor cortex stimulation: a combined transcranial magnetic stimulation/functional magnetic resonance imaging study. Cortex, What's your poison? Neurobehavioural consequences of exposure to industrial, agricultural and environmental chemicals 74, 134–148. https://doi.org/10.1016/j.cortex.2015.10.004.

Tingley, D., Yamamoto, T., Hirose, K., Keele, L., Imai, K., 2014. mediation: R package for causal mediation analysis. UCLA Stat. Stat, Assoc.
Tognoli, E., Kelso, J.A.S., 2014. The metastable brain. Neuron 81 (1), 35–48. https://doi.org/10.1016/j.neuron.2013.12.022.
Treynor, W., Gonzalez, R., Nolen-Hoeksema, S., 2003. Rumination reconsidered: a psychometric analysis. Cogn. Ther. Res. 27, 247–259. https://doi.org/10.1023/A:1023910315561.
Uher, R., Payne, J.L., Pavlova, B., Perlis, R.H., 2014. Major depressive disorder in DSM-5: implications for clinical practice and research of changes from DSM-IV. Depress. Anxiety 31 (6), 459–471. https://doi.org/10.1002/da.2014.31.issue-610.1002/da.22217.
Uhlhaas, P.J., Singer, W., 2006. Neural synchrony in brain disorders: relevance for cognitive dysfunctions and pathophysiology. Neuron 52 (1), 155–168. https://doi.org/10.1016/j.neuron.2006.09.020.
van der Knaap, L.J., van der Ham, I.J.M., 2011. How does the corpus callosum mediate interhemispheric transfer? A review. Behav. Brain Res. 223 (1), 211–221. https://doi.org/10.1016/j.bbr.2011.04.018.
Vanderhasselt, M.A., Kühn, S., De Raedt, R., 2011. Healthy brooders employ more attentional resources when disengaging from the negative: an event-related fMRI study. Cogn. Affect. Behav. Neurosci. 11 (2), 207–216. https://doi.org/10.3758/s13415-011-0022-5.
Váša, F., Shanahan, M., Hellyer, P.J., Scott, G., Cabral, J., Leech, R., 2015. Effects of lesions on synchrony and metastability in cortical networks. NeuroImage 118, 456–467. https://doi.org/10.1016/j.neuroimage.2015.05.042.
Wahl, M., Lauterbach-Soon, B., Hattingen, E., Jung, P., Singer, O., Volz, S., Klein, J.C., Steinmetz, H., Ziemann, U., 2007. Human motor corpus callosum: topography, somatotopy, and link between microstructure and function. J. Neurosci. 27 (45), 12132–12138. https://doi.org/10.1523/JNEUROSCI.2320-07.2007.
Walterfang, M., Wood, A.G., Barton, S., Velakoulis, D., Chen, J., Reutens, D.C., Kempton, M.J., Haldane, M., Pantelis, C., Frangou, S., 2009. Corpus callosum size and shape alterations in individuals with bipolar disorder and their first-degree relatives. Prog. Neuropsychopharmacol. Biol. Psychiatry 33 (6), 1050–1057. https://doi.org/10.1016/j.pnpbp.2009.05.019.
Watkins, E., Brown, R., 2002. Rumination and executive function in depression: an experimental study. J. Neurol. Neurosurg. Psychiatry 72, 400–402. https://doi.org/10.1136/jnnp.72.3.400.
Watkins, E.R., 2008. Constructive and unconstructive repetitive thought. Psychol. Bull. 134, 163–206. https://doi.org/10.1037/0033-2909.134.2.163.
Whitmer, A.J., Gotlib, I.H., 2013. An attentional scope model of rumination. Psychol. Bull. 139, 1036–1061. https://doi.org/10.1037/a0030923.
Wise, T., Marwood, L., Perkins, A.M., Herane-Vives, A., Joules, R., Lythgoe, D.J., Luh, W.-M., Williams, S.C.R., Young, A.H., Cleare, A.J., Arnone, D., 2017. Instability of default mode network connectivity in major depression: a two-sample confirmation study. Transl. Psychiatry 7 (4), e1105. https://doi.org/10.1038/tp.2017.40.
Yan, C.-G., Wang, X.-D., Zuo, X.-N., Zang, Y.-F., 2016. DPABI: data processing & analysis for (resting-state) brain imaging. Neuroinformatics 14, 339–351. https://doi.org/10.1007/s12021-016-9299-4.
Yu, J., Tseng, P., Hung, D.L., Wu, S.-W., Juan, C.-H., 2015. Brain stimulation improves cognitive control by modulating medial-frontal activity and preSMA-vmPFC functional connectivity. Hum. Brain Mapp. 36 (10), 4004–4015. https://doi.org/10.1002/hbm.22893.
Zalesky, A., Fornito, A., Bullmore, E.T., 2010. Network-based statistic: identifying differences in brain networks. NeuroImage 53 (4), 1197–1207. https://doi.org/10.1016/j.neuroimage.2010.06.041.
Zhang, C., Cahill, N.D., Arbabshirani, M.R., White, T., Baum, S.A., Michael, A.M., 2016. Sex and age effects of functional connectivity in early adulthood. Brain Connect. 6 (9), 700–713. https://doi.org/10.1089/brain.2016.0429.
Zhang, R., Jiang, G., Tian, J., Qiu, Y., Wen, X., Zalesky, A., Li, M., Ma, X., Wang, J., Li, S., Wang, T., Li, C., Huang, R., 2016. Abnormal white matter structural networks characterize heroin-dependent individuals: a network analysis. Addict. Biol. 21 (3), 667–678. https://doi.org/10.1111/adb.12234.
Zhang, R., Kranz, G.S., Lee, T.M.C., 2019. Functional connectome from phase synchrony at resting state is a neural fingerprint. Brain Connect. 9 (7), 519–528. https://doi.org/10.1089/brain.2018.0657.
Zhi, D., Calhoun, V.D., Lv, L., Ma, X., Ke, Q., Fu, Z., Du, Y., Yang, Y., Yang, X., Pan, M., Qi, S., Jiang, R., Yu, Q., Sui, J., 2018. Aberrant dynamic functional network connectivity and graph properties in major depressive disorder. Front. Psychiatry 9, 339. https://doi.org/10.3389/fpsyt.2018.00339.
Zuo, N., Fang, J., Lv, X., Zhou, Y., Hong, Y., Li, T., Tong, H., Wang, X., Wang, W., Jiang, T., Soriano-Mas, C., 2012. White matter abnormalities in major depression: a tract-based spatial statistics and rumination study. PloS One 7 (5), e37561. https://doi.org/10.1371/journal.pone.0037561.

Further reading

Fox, M.D., Snyder, A.Z., Vincent, J.L., Corbetta, M., Essen, D.C.V., Raichle, M.E., 2005. The human brain is intrinsically organized into dynamic, anticorrelated functional networks. Proc. Natl. Acad. Sci. 102, 9673–9678. https://doi.org/10.1073/pnas.0504136102.